Figure 10.4 shows the detection of a fetus in ultrasound. The image was smoothed with a Gaussian kernel before the detection was performed. This avoids some local minima, and together with the attraction force provided by the new term, allowed to detect an object with gaps in its boundary. The initial curve is closer to the object to be detected to avoid further possible detection of false contours due to local minima. Although this problem is significantly reduced by the new term incorporated in our geodesic model, it is not completely solved. This problem might be automatically solved using better stopping functions g or by higher values of c, the constant velocity. Another classical technique for avoiding some local minima is to solve the geodesic flow in a multiscale fashion.

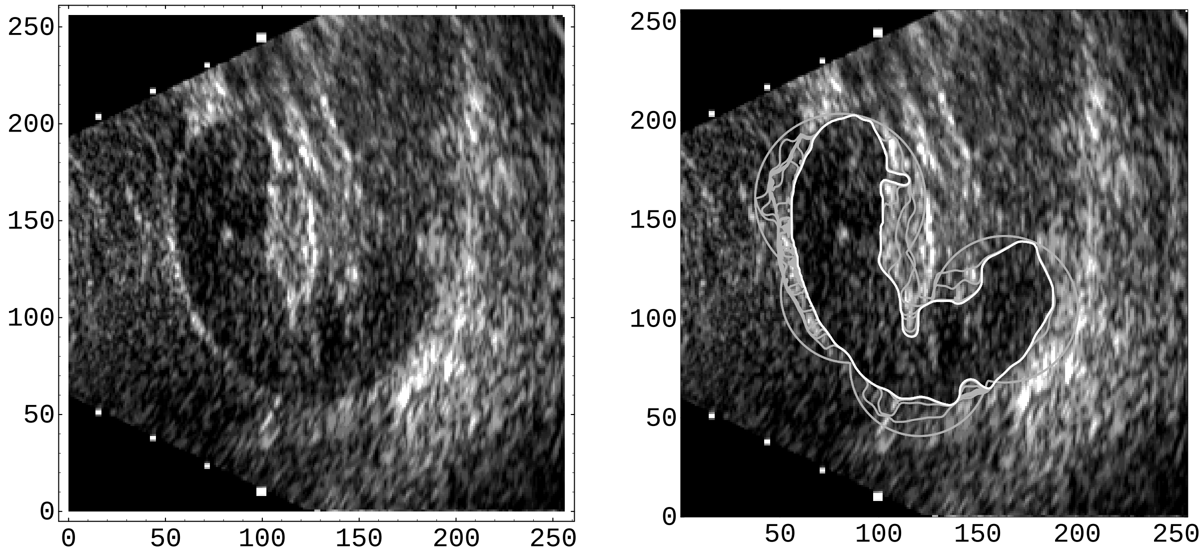

Figure 10.4: Object detection in an ultrasound image. The fetus is accurately detected by the geodesic active contours. In this case, the image was smoothed with a Gaussian kernel before the detection was performed.

10.4 Chapter Summary

A geodesic formulation of active contours was presented. It was shown that a particular case of the classical energy-snakes or active contours approach for boundary detection is equivalent to finding a geodesic curve in a Riemannian space derived from the image content. This proposes a new scheme for object boundary detection based on geodesic or minimal path computations. This approach also gives possible connections between classical energy based deformable contours and geometric curve evolution ones. The geodesic formulation introduced a new term to the curve evolution models that further attracts the deforming curve to the boundary, improving the detection of boundaries with large differences in their gradient. This term also partially frees the model from the need to estimate crucial parameters. Thereby, the geodesic formulation also improves previous approaches. The result is an active contour approach which is intrinsic (geometric) and topology independent. We also refer to the results regarding existence, uniqueness, stability, and consistency of the solution obtained by the proposed active contours. The experiments demonstrate the ability to detect several objects, as well as the ability to detect interior and exterior boundaries at the same time. The sub-pixel accuracy intrinsic to the algorithm allows to perform accurate measurements after the object is detected.

Extension of the $2D$ curve evolution model developed in [21, 95] is not straightforward, since an extension of the Euclidean heat flow was not yet developed. The geodesic formulation given by (10.3) can be extended to $3D$ replacing the $2D$ gradient by a $3D$ one and Euclidean arc-length (ds) by area [24].

Chapter 11

Edge Integration Using Minimal Geodesics

This chapter presents a new approach of edge integration for shape modeling [33]. Detection of the boundaries of objects in a given gray–level image is performed by a multi–stage procedure that integrates a potential generator and a weighted distance transform. This enables us to find the global minimum of the active contour model's energy proposed in the previous chapter. The proposed approach has an advantage over the classical snakes models since initialization becomes an easy task and the curve is not trapped at a local minimum. Applying the procedure enables the detection of object boundaries between two given points in cases of open boundaries like roads crossing the image domain, and closing a contour that models the boundary of an isolated object in the image, given only one point close to the objects' boundary. Closing contours is performed by using a topology–based saddle search routine. Examples of applying the proposed method to real images, typical for snakes applications, illustrate its performance.

11.1 Chapter Introduction

An active contour model for boundary integration and features extraction, introduced in [61], has been used and studied during the last years. Most of the approaches introduced since then try to overcome some of the main drawbacks of this model: *initialization, minimization and topology.*

The model requires the user to input an initial curve close to the desired goal. Often, it has to be a very precise polygon approximation and it may be fastidious to use for an application dealing with a large number of images. Using the balloon model [32] relaxes the initializations demands and almost any initial closed curve inside an object may be used to obtain its complete boundary. The same property is also obtained by using the geometrical methods [21, 94]. In [103], only two endpoints on the boundary are needed to follow the contour.

Although the smoothing effect of the snakes may overcome small defaults in the data, spurious edges generated by noise or in a complex image stop the evolution of the curve and it may be trapped at some undesired local minimum of the energy. The inflation or expansion force [32] prevents the contour from being trapped by isolated edges into an insignificant local minimum.

For segmenting several objects simultaneously or isolating an object with holes, it is possible [21, 94] to model the contour as a level set of a surface allowing the propagating contour to change its topology without external procedures that monitor these changes, see Chapter 2.

We present a new approach to find the global minimum for energy minimizing curves by giving only two end points. Our goal is to help the user in solving the problem in hand by mapping it into a single minimum problem. The proposed method contributes to the improvement of the first two items above (which are obviously related) since only endpoints are needed as initialization and the global minimum is found between these points. Using an approach of minimal path estimation on a surface [65], we give an evolution scheme that provides at each image pixel an output of the energy along the minimal path joining that pixel to the start point. The search for a global minimum is then done efficiently. While this minimum is restricted to start and end between two given points, we also present a topology–based saddle search that helps in automatically closing contours by clicking on a single point along the boundary. We stress the fact that the proposed algorithm is based on a search for the global minimum and may therefore lead to meaningless classifications in some cases. Yet, since the whole process is controlled by the user, such pathological cases may be easily avoided.

Section 11.2 explores the relation of deformable models to the proposed solution. A formal definition of our edge integration procedure for the shape modeling problem is given in Section 11.3. Section 11.4 presents some results of applying the proposed procedure to real images.

11.2 Active Contour Evolution

11.2.1 Energy minimization

The inherent difficulty in active contour models is that searching for a minimum over a non convex functional is possible only under predefined limitations that lead to the desired solution. One such possibility is allowing the user to specify an initial guess that is close, in some sense, to a local minimum. Starting from the user selection, like an initial given contour, a minimization scheme refines the initial guess to fit the given image data. Searching for the global minimum of the given functional does not necessarily make sense and initial and boundary conditions are important in the process of locating the desired local minimum. Searching for a global minimum is meaningless in the case of free end points or closed curves, since in both cases, the curve can vanish into a single point achieving a global minimum of the potential (0). In other cases, where some points are known to be part of a contour, given as fixed endpoints or as a constraint for a closed curve to pass through, it may be more reasonable to search for a global minimum.

To motivate the proposed solution let us first explore the relation to the classical active contour model. Deformable models are often used to integrate boundaries and extract features from images. The extraction of local features is specified by initial conditions that lead to the selection of one of the local minima. Snakes are a special case of deformable models as presented in [139]. The deformable contour model is a mapping:

$$\begin{aligned} \mathcal{C}(v) : \Omega \longrightarrow & \quad \mathbb{R}^2 \\ v \longmapsto & \quad (x(v), y(v)) \end{aligned} \tag{11.1}$$

where $\Omega = [0, 1]$ is the parameterization interval. In some cases v is chosen to be the arc-length parameter, and then $\Omega = [0, L]$ where L is the length of the curve. In some other cases, like periodic closed curves, $\Omega = S^1$ is the unit circle (in this case the parameter v is a mapping from the unit circle to the curve). The deformable model is a space of admissible deformations $\mathcal{A}$ and a functional E. This functional represents the energy of the model which will be minimized on $\mathcal{A}$ and has the following form:

$$\begin{aligned} E : \quad & \mathcal{A} \to \mathbb{R} \\ \mathcal{C} \mapsto E(\mathcal{C}) \quad & = \int_\Omega w_1 |\mathcal{C}_v(v)|^2 + w_2 |\mathcal{C}_{vv}(v)|^2 + P(\mathcal{C}(v)) dv \end{aligned} \tag{11.2}$$

where $\mathcal{C}_v$ and $\mathcal{C}_{vv}$ are the first and second derivatives of $\mathcal{C}$ with respect to v, and P is the potential associated to the external forces. The potential is computed as a function of the image data according to the desired goal. If, for example, we want the snake to be attracted to edge points, the potential should depend on the image gradient. Usually the space of admissible deformations $\mathcal{A}$ is restricted by boundary conditions $\mathcal{C}(0)$, $\mathcal{C}_v(0)$, $\mathcal{C}(1)$ and $\mathcal{C}_v(1)$ being given, or by using periodic closed curves. The mechanical properties of the model are controlled by the functions w_j.

If $\mathcal{C}$ is a local minimum of E, it satisfies the associated Euler-Lagrange equation:

$$\begin{cases} -(w_1 \mathcal{C}_v)_v + (w_2 \mathcal{C}_{vv})_{vv} + \nabla P(\mathcal{C}) = 0 \\ \text{given boundary conditions.} \end{cases} \tag{11.3}$$

In this formulation each term appears as a force applied to the curve. A solution can be viewed either as realizing the equilibrium of the forces in the equation or as reaching the minimum of the energy. Thus the curve is under the control of two types of forces:

- The internal forces (the first two terms) which impose the regularity of the curve. The choice of constants w_1 and w_2 determines the elasticity and rigidity of the curve.

- The image force (the potential term) pushes the curve to the significant lines which correspond to the desired attributes. It is defined by a potential of the form $\int_0^1 P(\mathcal{C}(v))dv$ where

$$P(\mathcal{C}) = g(|\nabla I(\mathcal{C})|). \tag{11.4}$$

Here, I denotes the image and $g(\cdot)$ is a decreasing function, see [30] for several possibilities of selecting a potential function. The curve is then attracted by the local minima of the potential, i.e. edges (see [47] for a more complete discussion of the relationship between minimizing the energy and locating contours). Other forces can be added to impose constraints defined by the user. In our problem the initial data is often the set of points generated by an edge detection operator [20]. As introduced in [32], previous local edge detection might be taken into account for defining the potential. Many approaches of generating 'attractions potentials' from such data for various reconstruction methods were surveyed in [30].

A geometric approach for deformable models was recently introduced in [95, 21]. A level set approach for curve evolution [111, 127] is used to implement a planar curve evolution of the form:

$$\frac{\partial \mathcal{C}(s,t)}{\partial t} = P(\mathcal{C})(\mathcal{C}_{ss} + w\mathcal{N}) \tag{11.5}$$

where s is the arc-length parameter of the curve $\mathcal{C}$ in this case. Therefore, $\mathcal{C}_{ss} \equiv \kappa\mathcal{N}$ is the curvature vector ($\mathcal{N}$ being the unit normal), and w is some predefined constant. It was shown that the geometric snakes model performs better than the classical snakes in some cases. It was recently shown that introducing the 'gradient of potential' (∇P) term of the classical energy minimization snakes [61, 30, 90] into the geometric snakes [95, 94, 21] is based on geometrical as well as energy minimization reasoning, leading to the "geodesic active contours." The geodesic active contours [23] were proven to 'behave' better than both its 'ancestors', as shown in Chapter 10. However, in all these approaches, the algorithms search for some local minimum that is close to the initial guess while we propose a method for finding the global minimum.

11.3 Paths of Minimal Action

Given some potential P that takes lower values near the edges, our goal is to find a single contour that best fits the boundary of a given object. This 'best fit' question leads to algorithms seeking for the minimal path in the sense of the potential P (i.e. paths along which the integration over P is the minimal, as presented in the previous section with snakes.) As mentioned earlier, snakes start from a path close to the solution and converge to a local minimum of the energy. Our goal is to make the initialization task easier by giving only the end points and then find the minimal path between these points. At first glance, this limits the problem to the type of boundary conditions with fixed end points, however, we will see in Section 11.3.5 that the proposed approach may also be used for closed contours. We use the ideas developed in [65, 76] to determine the shortest path between two points on a given surface and the fact that a weighted distance transform [118, 76, 141] operating on a given potential function helps in finding the solution for our path of minimal action (also known as minimal geodesic, or path of minimal potential), and thereby, in isolating the boundary of a given object in the image.

11.3.1 Distance potential

Let us first introduce some notations. Let $I(x,y) : D \in \mathbb{R}^2 \to \mathbb{R}^+$ be a given gray level image. Applying a standard edge detector to I results in a set of points in the image domain (D) some of which correspond to true edge points. These points are scattered over the image domain and serve as the key points in generating a single boundary contour. Finding such a contour is usually referred to as 'shape modeling' that is used for object segmentation and classification [95, 94, 93].

Denote $\mathcal{E}(x,y) : D \to \{0,1\}$ a binary function representing the result of applying a standard edge detector on the image I, where 1 corresponds to a detected edge point. One possible way of defining a potential $P : D \to \mathbb{R}^+$ is the distance map [30], where each point p is assigned with a value representing the shortest Euclidean distance to an edge point:

$$P(p) = \inf_{\mathcal{E}(q)=1} \{d(p,q)\} \tag{11.6}$$

where $d(p,q)$ is the Euclidean distance between the two points p and q. Consistent numerical approximations of (11.6) for the computation of P on a sequential computer involves in high complexity. Quick sequential algorithms [10, 37] were used for defining the attraction potential in [30]. However, sub-pixel estimation of the distance using a parallel algorithm was presented in [76]. It gives a high *sub-pixel* precision of the distance, as presented in Chapter 3. This is only one possible selection of P for shortest path estimation [65, 137] presented briefly in the next section. In some of the examples, we have chosen the potential to be the gray-level image itself.

11.3.2 Shortest paths on graph surfaces

Let $\mathcal{S} \subset \mathbb{R}^3$ be a given surface that represents the graph of some real function on the plane. In Chapter 6 [65], a method to determine the shortest path on this surface between a starting point x_S and a destination x_D was presented. It was shown that the projection on the plane of the level set curves of the geodesic distance on $\mathcal{S}$ to x_S can be obtained using a simple curve evolution scheme. Using the Osher-Sethian approach for front propagation, the distance function $\mathcal{M}_S$ to x_S on $\mathcal{S}$ is defined by the projection on $\mathbb{R}^2$ of its level sets which are shown to be identical to the evolving zero level sets of the function $\phi : \mathbb{R}^2 \times [0,T) \to \mathbb{R}$ defined by the evolution equation:

$$\frac{\partial \phi}{\partial t} = V_N |\nabla \phi|. \tag{11.7}$$

where V_N is defined by local properties of the surface $\mathcal{S}$ and ϕ.

The geodesic distance function $\mathcal{M}_D$ to x_D on $\mathcal{S}$ is computed in the same way. Then the minimal geodesic path between x_S and x_D is exactly the set of points x_g that satisfy

$$\mathcal{M}_S(x_g) + \mathcal{M}_D(x_g) = \inf_{x \in \mathbb{R}^2} \{\mathcal{M}_S(x) + \mathcal{M}_D(x)\} \tag{11.8}$$

A similar approach is used in [76] and in Chapter 3 to define a weighted distance transform and the path of minimal cost by defining $V_N = \frac{1}{P}$ in Equation (11.7). We apply these ideas to our problem of finding curves of minimal action from the potential data.

11.3.3 Problem formulation

The minimization problem we are trying to solve is slightly different from the deformable models, though there is much in common. The energy of the new model has the following form:

$$\begin{aligned} E: \quad & \mathcal{A} \to \mathbb{R} \\ & \mathcal{C} \mapsto E(\mathcal{C}) = \int_\Omega w + P(\mathcal{C}(s))ds = \int_\Omega \tilde{P}(\mathcal{C}(s))ds \end{aligned} \tag{11.9}$$

Here $\mathcal{A}$ is the space of all curves connecting two given points (restriction by boundary conditions): $\mathcal{C}(0) = p_0$ and $\mathcal{C}(L) = p_1$, where L is the length of the curve. Contrary to the classical snake energy, here s represents the arc-length parameter. This makes the energy depend only on the geometric curve and not on the parametrization (see [22]). The regularization term with w now exactly measures the length of the curve. We note that a similar regularization effect may be also achieved by smoothing the potential P.

To simplify our discussion consider the potential to be a distance map of an edge detection (Equation. (11.6)). Note also that the distance potential selection may be also considered as the normalized force introduced in [32] for stabilizing the results (*i.e.* $\nabla \hat{P} = \frac{\nabla P}{|\nabla P|}$) since $|\nabla \hat{P}| = 1$.

Having the above minimization problem in mind, we first search for the *surface of minimal action* starting at $p_0 = \mathcal{C}(0)$. This is the surface giving as an altitude: At each point p of the image plane the value corresponds to the minimal energy of a path starting at p_0 and ending at p. Following [65], it is possible to formulate a partial differential evolution equation describing the set of equal energy contours $\mathcal{L}$ in 'time'. The evolution equation is of the following form:

$$\frac{\partial \mathcal{L}(s,t)}{\partial t} = \frac{1}{\tilde{P}} \vec{n}(s) \tag{11.10}$$

where $\tilde{P} = P + w$ and $\vec{n}(s)$ is the normal to the closed curve $\mathcal{L}(s,t) : S^1 \times [0,T) \to \mathbb{R}^2$. This evolution equation is similar to a balloon evolution [32] with an inflation force depending on the point of the curve. The curve $\mathcal{L}(s,t)$ corresponds here to the set of points r for which the minimal energy is t:

$$\{\mathcal{L}(s,t), s \in S^1\} = \{r \in \mathbb{R}^2 \mid t = U(r) = \inf_{\mathcal{A}_r}(\int_{\tilde{\mathcal{C}}} \tilde{P} d\tau)\} \tag{11.11}$$

where $\mathcal{A}_r$ is the set of all planar curves $\tilde{\mathcal{C}}$ connecting the points p_0 and r, and τ is the arc-length parameter of $\tilde{\mathcal{C}}$. This evolution equation is initialized by a curve $\mathcal{L}(s,0)$ which is an infinitesimal circle surrounding the point p_0. It corresponds to a null energy. Considering the (x, y, t)-space, the family of curves $\mathcal{L}(s, t)$ appear to be the level sets of the surface $U(x, y) : \mathbb{R}^2 \to \mathbb{R}^+$ defined in (11.11) for which the level set $\{(x, y)|U(x, y) = t\}$ corresponds to the curve $\mathcal{L}(s, t)$.

It is possible to compute the surface U in several ways. We shall describe two of them that are consistent with the continuous case while implemented on a rectangular grid. It is, however, possible to implement a simple 'weighted distance transforms' like the shading from shape algorithm introduced in [141], if consistency with the continuous case is not important, see also [118].

Osher-Sethian front propagation approach

According to the first approach the curve evolution $\mathcal{L}(t)$ is reformulated into an evolution of an implicit representation of the curve defined by an evolving surface $\phi : \mathbb{R}^2 \times [0, T) \to \mathbb{R}$, where $\mathcal{L} = \phi^{-1}(0)$. This means that curve $\mathcal{L}(t)$ is the zero level set of $\phi(t) : \mathbb{R}^2 \to \mathbb{R}$. See Chapter 2. The $\phi(0)$ function is initialized to be negative in the interior and positive in the exterior of the curve $\mathcal{L}(0)$. The evolution rule of ϕ is then given by:

$$\frac{\partial \phi}{\partial t} = \frac{1}{\tilde{P}} |\nabla \phi|. \tag{11.12}$$

It was this same idea of considering the curve as the zero level set of an evolving surface that initiated the geometric snake approach [95, 21] described in the end of Section 11.2.

Rouy-Tourin shape from shading approach

The second approach is based on a shape from shading method [117] and searches for the surface U itself instead of tracking its level sets. In this case the surface may be found according to the following minimization procedure:

$$\frac{\partial U}{\partial \tau} = \tilde{P} - |\nabla U|, \tag{11.13}$$

Here, boundary conditions are given in the form of fixing the point $p_0 = \mathcal{C}(0)$, i.e. $U(p_0, \tau) = 0$. Authors of [117] gave a convergence proof to that minimization procedure in the viscosity solutions framework [36]. An efficient sequential algorithm (Gauss-Seidel) for solving the above problem may be found in [42].

Selecting between the proposed numerical methods for computing the weighted distance transform is a delicate issue. One must consider efficiency, robustness (stability) and accuracy. The algorithms in hand vary from sequential type that scan the image upside-down left to right and then backwards (bottom-up right to left) for several few iterations, to parallel type of algorithms and robust level set propagation type of algorithms. We note that the number of scans of the image required by a sequential algorithm depends on the behavior of the most complicated geodesic path.

11.3.4 Global snake minimization between two end points

Using the approach of [65] described in Section 11.3.2, the shortest path between a starting point p_0 and a destination point p_1, according to the energy minimization is the set of points (x_m, y_m) that satisfy:

$$U_0(x_m, y_m) + U_1(x_m, y_m) = \inf_{(x,y)} \{U_0(x, y) + U_1(x, y)\} \tag{11.14}$$

where U_0 and U_1 correspond to the minimal action obtained from the previous section with paths starting at p_0 and p_1 respectively. We remark that in order to determine this minimal path between p_0 and p_1, we need only to calculate U_0 and then slide on the surface U_0 from p_1 to p_0. Indeed, the surface of minimal action U_0 has a convex like behavior in the sense that starting from any point q in the image domain and following the gradient descent direction we will always converge to p_0. It means that U_0 has only one local minimum that is of course the global minimum and is reached at p_0. We show in Figure 11.7a an example of 3D representation of the $U_0(x, y)$ surface and a level set image of the same U_0. It is therefore possible to extract the desired contour directly by using a simple back tracking algorithm. Given the point p_1, the path of minimal action connecting p_0 (the minimal point in U_0, $U(p_0) = 0$) and p_1 is the curve starting at p_1 and following the opposite gradient direction on U_0. The back propagation procedure is a simple steepest gradient descent. Implemented on a rectangular grid, given a point $q = (i, j)$, the next point in the chain connecting q to p is selected to be the grid neighbor (k, l) for which $U(k, l)$ is the minimal, and so forth. We thereby track the path of minimal action connecting the two points. This is the global minimum of the snake energy defined in . (11.9).

11.3.5 Closed boundary extraction from a single point

It is often needed to detect a closed contour. Our previous approach of finding a minimal path between two given endpoints detects the two paths that complete a closed contour only if both ways correspond to a global minimum. In the general case of selecting the second point, it is clear that although both ways are local minima, only one is a global minimum. However, assuming only one starting point p_0 is given on the closed contour, we compute the minimal action U from this starting point. We should then find a second point p_1 that is located on the unknown contour and from where the two half paths have the same energy. This means we have to find a point p_1 from where there is more than one curve connecting it to the source p_0. These special points are the saddles of U. The saddle points may serve as clues in closing contours of objects that are contained within the image domain. When the user searches for a closed contour from p_0, a search for saddle points on U is performed. Back propagating from a saddle point p_1 to both directions will connect the saddle to the source point p_0 by two curves. Thereby, a closed contour is formed representing the complete boundary of an object. It is possible to isolate the saddle points on U by using a simple test to determine the number of *level crossings*.

Consider a small radius circle centered at a candidate point q and embedded in the horizontal plane $(x, y, U(q))$. Denote the number of level crossings as the number of points this circle intersects with the surface $(x, y, U(x, y))$. It is shown in Figure 11.1 that this number at a saddle point is equal to four, while for most surface points it is two, and at maximum and minimum points there are no level crossings. Although there are only few saddle points in U (see Figure 11.7c for example), finding the level crossing for every point q in the domain is not enough. It is necessary to filter out the insignificant saddles. Selecting the right regularization constant w will filter out most of the saddles that are formed due to noise.

In our implementation of the number of level crossings, for each point (i, j) in the pixels grid, we simply count the number of sign changes in $U(k, l) - U(i, j)$ while traveling around the 8 neighbors (k, l) of the point.

According to our experience selecting the right w (large enough for a smoothing effect) reduced the number of saddles to the only interesting ones. However, since we are dealing with a user interactive procedure, it is possible to paint the candidate saddle points on the image for the user to decide. Selecting the right saddle point will close the contour and segment the object.

In a favorable case where there are not much gaps in the boundary contour, an alternative criteria that will do the work is to consider only those saddle points that are close to edge points, since it is obvious that the contour should pass close to an edge.

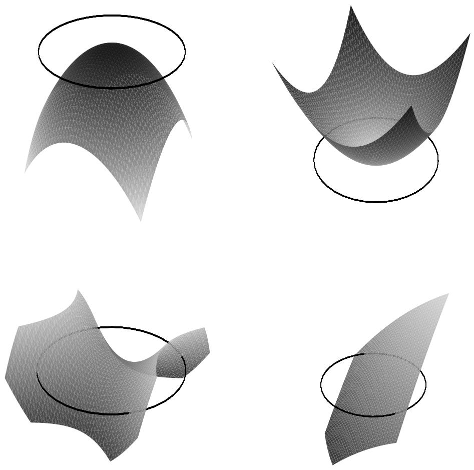

Figure 11.1: Illustrating the number of level crossings. At the top, a maximum and a minimum points give 0, at the bottom left, a saddle point gives 4, and at the bottom right, other points give 2 level crossings.

11.4 Examples and Results

We demonstrate the performance of the proposed algorithm by applying it to several real images. The images were scaled to 128×128 pixels.

In the first example, we are interested in a road detection between two points in the image of Figure 11.2. Road areas are lighter and correspond to higher gray levels. The potential function P was thus selected to be the opposite of the gray level image itself: $P = -I$. In Figure 11.4, we compare between the proposed method and the classical snakes with two different initializations. At the top example the classical snake is trapped into a local minimum and requires a very accurate initial guess, as in the middle example, to guarantee convergence to the desired solution. It is shown that given two end points, the proposed procedure detects the path of minimal action along the right road. We show in Figure 11.3 the image of $U(x,y)$. Observe the way the level curves propagate faster along the road.

Figure 11.2: Original Road Image

Note, that using a completely different approach, the authors of [103] also found a way to solve better the problem of finding a minimal energy path between two end points. Using the same road image, Figure 11.5 presents two examples for which their method leads to a local minimum. Taking the same end points as in Figure 11.4, the part of curve close to the upper right end point is trapped by the white building below it, like in the upper example of Figure 11.4. If the end point is slightly shifted, the curve follows the road correctly from both ends but at some time, it prefers a short-cut. Note, that in both examples we do not present the final curve position but its position at some intermediate time from which it is not possible to return back to the correct road.

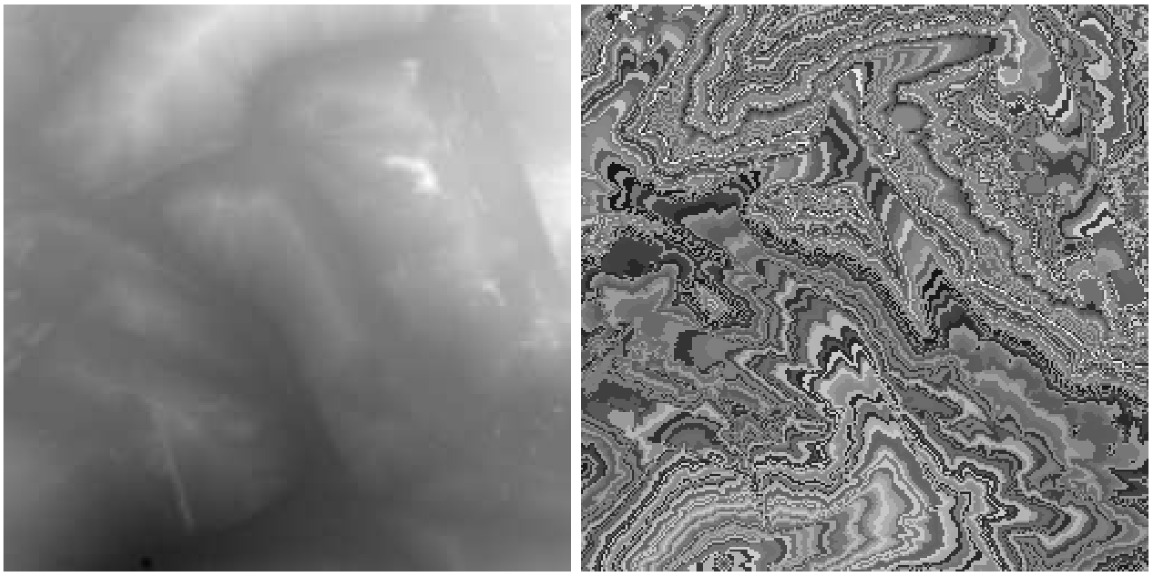

Figure 11.3: Minimal action U from bottom left starting point. On the left, black corresponds to lower values of U, on the right a random look up table is used to render the level curves of U.

In the second example, we want to extract the left ventricle in an MR image of the heart area. The potential is a function of the distance to the closest edge in a Canny edge detection image (see Figure 11.6). Since it is a closed contour we use the saddle points classification helping in closing boundaries of a single object in the heart image (see Figure 11.7).

11.5 Chapter Summary

In this chapter we presented a method for integrating objects boundaries by searching for the path of minimal action connecting two points. The search for the global minimum makes sense only after the two end points are determined, and the 'action' or 'potential' is generated from the image data. This makes the snake initialization easier needing only two points and avoids the active contour model being trapped in a local minimum. Applying the proposed procedure to real images gave better results in these cases than previous approaches. The result of the proposed procedure may be considered either as a final solution or as initial condition for classical snake models for further smoothing. Convergence to the proper smoothed version should now be almost immediate, since the global minimum should be close to its smoothed version obtained by a classical snake.

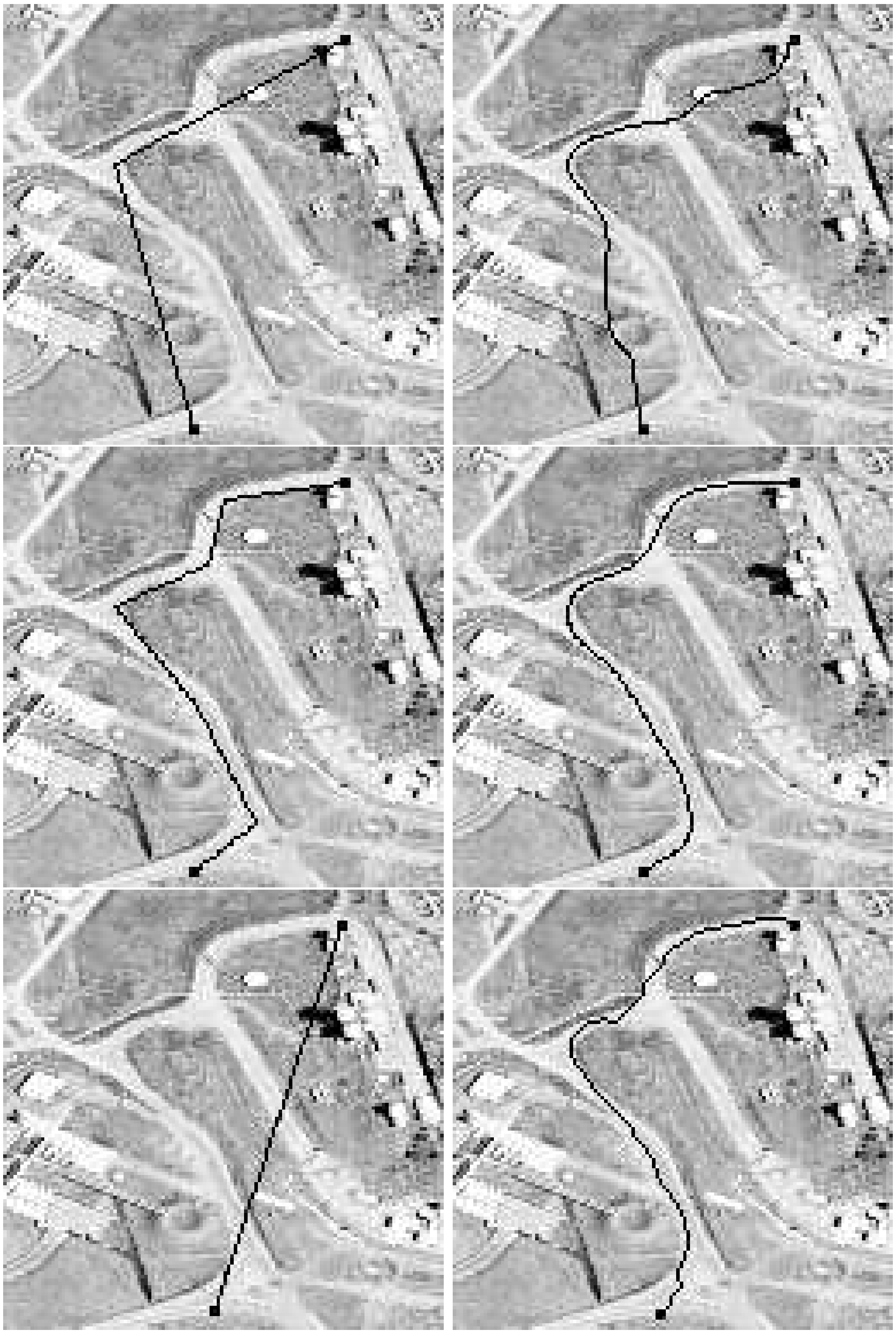

Figure 11.4: Comparing classical snakes and the proposed approach. The initial data is shown on the left and the result on the right. The top and middle show the results of two different initializations of the classical snakes. The bottom example shows our path of minimal action connecting the two black points as start and end points.

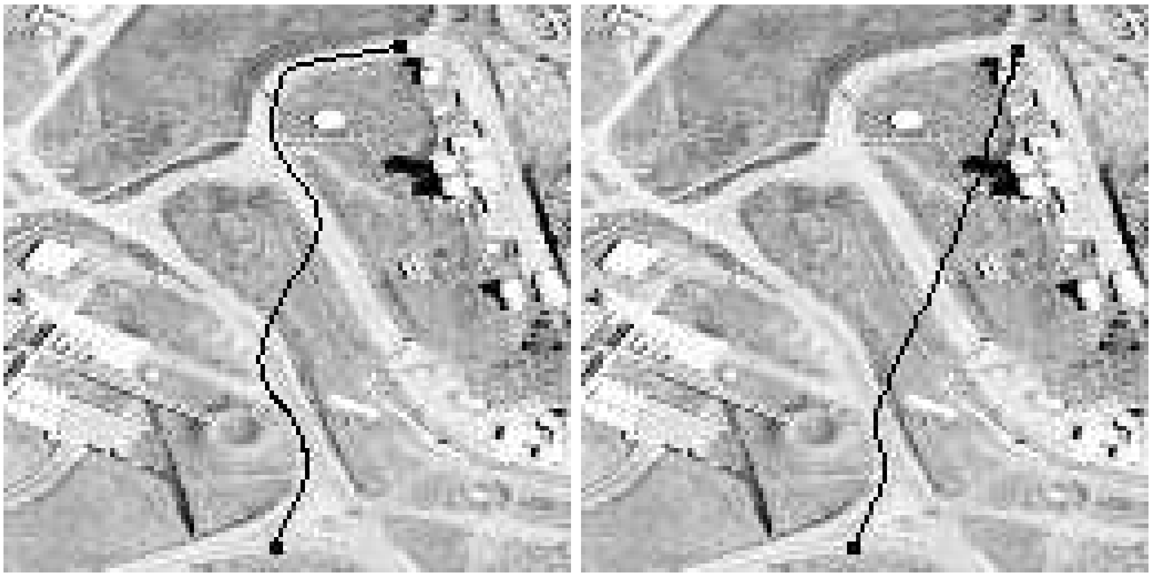

Figure 11.5: Two examples of applying the approach of [103] with two slightly different initializations. In both cases the curve is trapped into a local minimum.

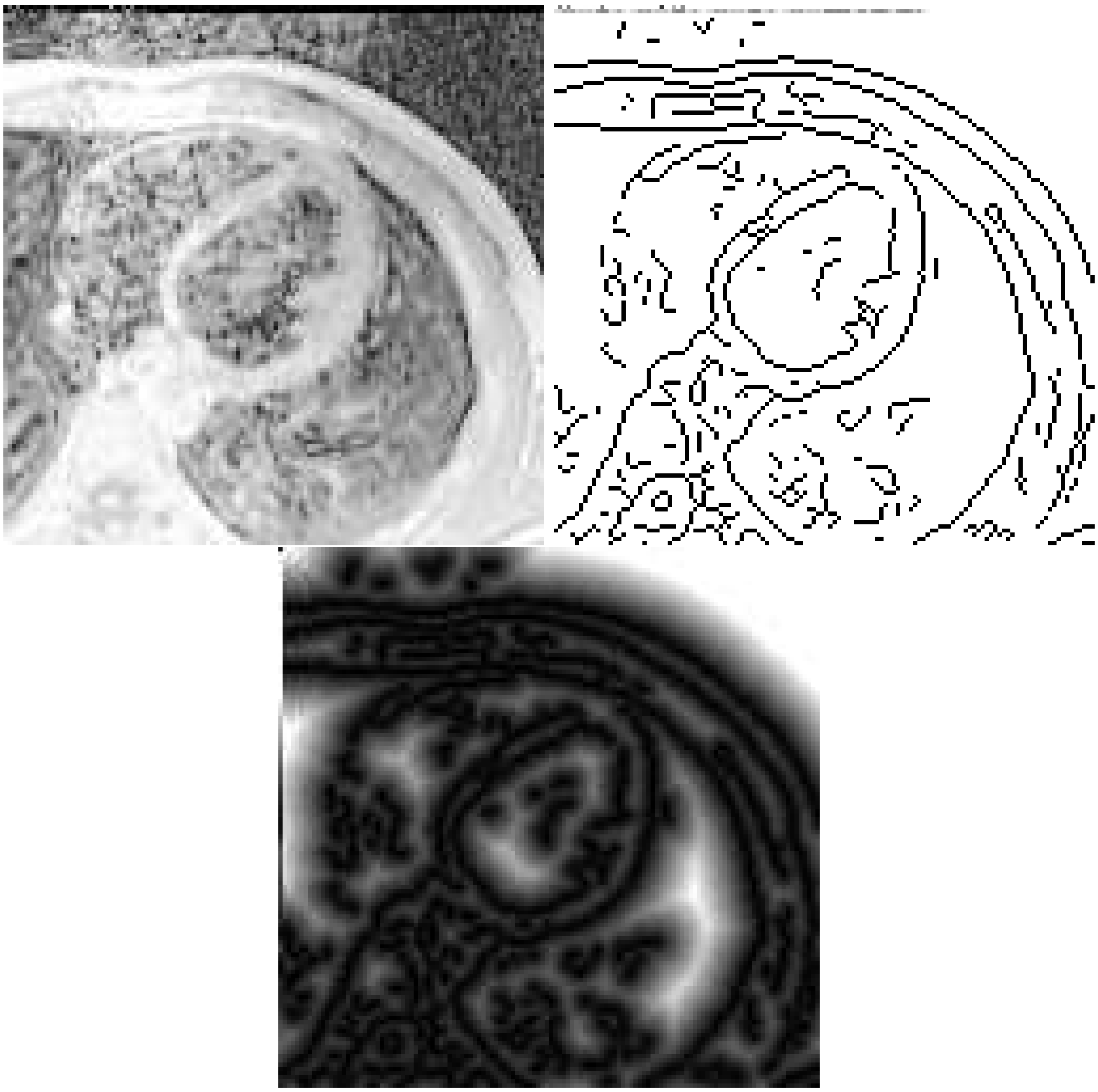

Figure 11.6: MRI heart image: Original image on the top left, edge image on the top right, distance map on the bottom.

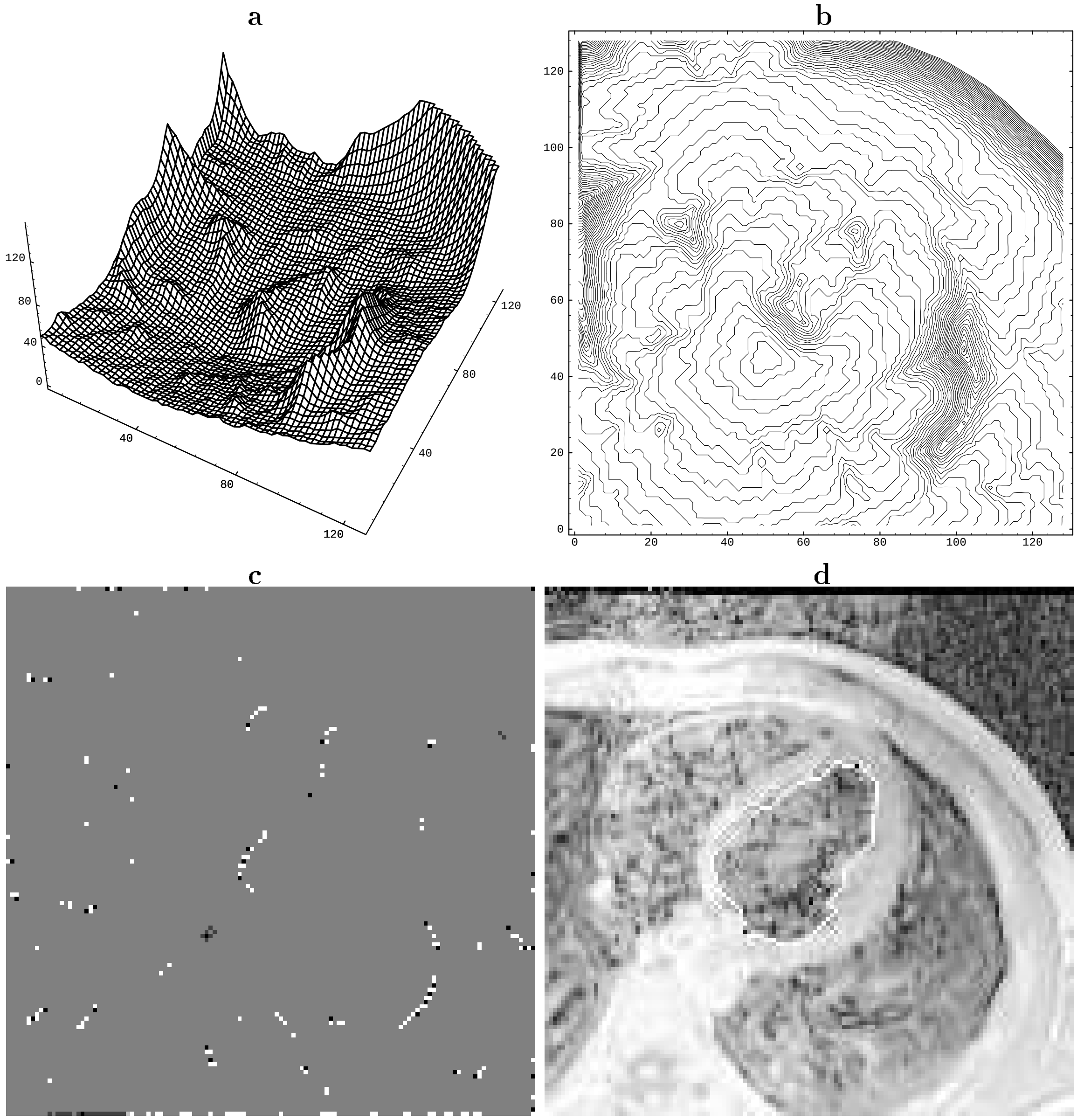

Figure 11.7: MRI heart image: minimal action U representation as a graph surface in (**a**) and its level set curves (**b**). The start point is the lower point ($U = 0$) located on the bottom left of the ventricle at pixel (48,44). The process of the heart ventricle detection goes as follows: To find the second end point, saddle point classification is used on (**c**). The number of level crossings appears in black for 0 (maxima and the minimum), gray for 2 (most of the points) and white for 4 (saddle). After filtering the white pixels, the selected saddle point is used to find the two half contours on (**d**). The contour is white and the two end points are the two black pixels. The starting point is on the lower left and the other is the detected saddle.

Chapter 12

Summary and Outlook

In this thesis, curve evolution and level set propagation were explored. Classical problems like Shape from Shading in computer vision and Navigation among Moving Obstacles in robotics, were addressed by finding the right curve evolution equation that describes the problem. Then, the curve evolution equations were reformulated into Eulerian formulations and Osher-Sethian based numerical algorithms were used to propagate the curves efficiently and accurately. The projection of propagating curves on surfaces to the natural (x, y) parametric plane, helped in tracking their location and considerably reduced the complexity involved in numerical implementations aimed at simulating these evolutions.

The level set way of thinking led us to the solutions of the global shape from shading problem, the Steiner problem, to the construction of the global skeletonization algorithm, and to the design of Voronoi diagrams on surfaces. The search for geometrical local and minimal geodesics, directed us towards the construction of the geodesic active contours and the edge integration algorithms for shape modeling and segmentation.

Our feeling is that there are still many problems out there starving for the curve evolution solution and the Eulerian formulation implementation. The direct relation between curve evolution and integration makes curve evolution techniques a powerful tool for many engineering problems. Our hope is that our small contribution in this field will open the door to this direction.

From the practical point of view, the numerical algorithms we dealt with are very efficient when implemented on parallel machines. Indeed, the local nature of the Eulerian formulations lends itself to parallel implementations. Until parallel computers are commonly available, sequential versions of the proposed algorithms should be devised. However, when considering sequential algorithms one should remember that it is the process of curve evolution that we are after, and though the final curve position is important, the different positions of the propagating curve in time are all part of the solution. Moreover, the consitency with the continuous case is an important peoperty that guarantees that the numerical scheme converge to the continuous case as the discretization grid is refined. These two important properties that should be sattisfied, make the search for sequantial schemes a non-trivial task.

From a theoretical point of view, there are still open questions in curve and surface evolution. One important question is whether a '$3D$ geometric heat equation' exists, *i.e.* a local geometric property that shrinks any given $3D$ shape that is homeomorphic to a sphere into a sphere. Our feeling is that such an evolution does not exist, yet a theoretical proof for that is still missing. It is however possible to overcome this theoretical void for $3D$ deformable surfaces that are used for $3D$ segmentation. This is one of the directions in our future research.

Bibliography

[1] E Adin and A M Bruckstein. Navigation in a dynamic environment. Center for Intelligent Systems Report CIS #9101, Technion–Israel Institute of Technology, Israel, January 1991.

[2] L Alvarez, F Guichard, P L Lions, and J M Morel. Axioms and fundamental equations of image processing. *Arch. Rational Mechanics*, 123, 1993.

[3] C Arcelli. Pattern thinning by contour tracing. *CGIP*, 17:130–144, 1981.

[4] C Arcelli and G Sanniti di Baja. A width independent fast thinning algorithm. *IEEE Trans. on PAMI*, 7:463–474, 1985.

[5] J M Beck, R T Farouki, and J K Hinds. Surface analysis methods. *IEEE CG&A*, pages 18–37, December 1986.

[6] M Bichsel and A P Pentland. A simple algorithm for shape from shading. In *Proceedings IEEE CVPR*, pages 459–465, Champaign, Illinois, May 1992.

[7] H Blum. A transformation for extracting new descriptors of shape. In Walthen Dunn, editor, *Models for the Perception of Speech and Visual Form*, pages 362–380. MIT Press., 1967.

[8] H Blum. Biological shape and visual science (part I). *J. theor. Biol.*, 38:205–287, 1973.

[9] F L Bookstein. The line skeleton. *CGIP*, 11:123–137, 1979.

[10] G Borgefors. Distance transformations in arbitrary dimensions. *CVGIP*, 23:321–345, 1984.

[11] J W Brandt. Convergence and continuity criteria for discrete approximations of the continuous planar skeleton. *CVGIP: Image Understanding*, 59:116–124, 1994.

[12] J W Brandt and V R Algazi. Continuous skeleton computation by voronoi diagram. *CVGIP: Image Understanding*, 55:329–338, 1992.

[13] R W Brockett and P Maragos. Evolution equations for continuous–scale morphology. In *Proceedings IEEE international Conference on Acoustics, Speech, and Signal Processing*, pages 1–4, San Francisco, California, March 1992.

[14] M J Brooks and W Chojnacki. direct computation of shape from shading. In *Proceedings of ICPR, International Conference of Pattern Recognition*, pages 114–119, Jerusalem, Israel, October 1994.

[15] J W Bruce and P J Giblin. *Curves and Singularities*. Cambridge University Press, 1992. 2-nd Edition.

[16] A M Bruckstein. On shape from shading: Some theoretical considerations. EE Report 524, Technion–Israel Institute of Technology, June 1985.

[17] A M Bruckstein. On shape from shading. *Comput. Vision Graphics Image Process.*, 44:139–154, 1988.

[18] A M Bruckstein. Analyzing and synthesizing images by evolving curves. In *Proceedings IEEE ICIP*, volume 1, pages 11–15, Austin, Texas, November 1994.

[19] L Calabi and W E Hartnett. Shape recognition, prairie fires, convex deficiencies and skeletons. *Am. Math. Mon.*, 75:335–342, 1968.

[20] J Canny. A computational approach to edge detection. *IEEE Trans. on PAMI*, 8(6):679–698, 1986.

[21] V Caselles, F Catte, T Coll, and F Dibos. A geometric model for active contours. *Numerische Mathematik*, 66:1–31, 1993.

[22] V Caselles, R Kimmel, and G Sapiro. Geodesic active contours. *submitted*, 1994.

[23] V Caselles, R Kimmel, and G Sapiro. Geodesic active contours. In *Proceedings ICCV'95, to appear*, Boston, Massachusetts, June 1995.

[24] V Caselles, R Kimmel, C Sbert, and G Sapiro. Three dimensional object segmentation via minimal surfaces and geometric deformable modelse. *submitted*, 1995.

[25] Y G Chen, Y Giga, and S Goto. Uniqueness and existence of viscosity solutions of generalized mean curvature flow equations. *J. Diff. Geom.*, 33, 1991.

[26] D L Chopp. Computing minimal surfaces via level set curvature flow. Ph.D Thesis, Lawrence Berkeley Lab. and Dep. of Math. LBL-30685, Uni. of CA. Berkeley, May 1991.

[27] D L Chopp. Flow under geodesic curvature. Dept. of Mathematics Report 92-23, UCLA, 1992.

[28] D L Chopp. Computing minimal surfaces via level set curvature flow. *J. of Computational Physics*, 106(1):77–91, May 1993.

[29] D L Chopp and J A Sethian. Flow under mean curvature: Singularity formation and minimal surfaces. Center for pure applied math. pam-541, Univ. of CA. Berkeley, November 1991.

[30] I Cohen and L D Cohen. Finite element methods for active contour models and balloons for 2-D and 3-D images. *IEEE Trans. on PAMI*, 15(11), 1993.

[31] I Cohen, L D Cohen, and N Ayache. Using deformable surfaces to segment 3d images and infer differential structure. *CVGIP*, 56, 1992.

[32] L D Cohen. On active contour models and balloons. *CVGIP: Image Understanding*, 53(2):211–218, 1991.

[33] L D Cohen and R Kimmel. Edge integration using minimal geodesics. EE PUB No. 952, Technion–Israel Institute of Technology, Israel, January 1995. submitted.

[34] R Courant, K O Friedrichs, and H Lewy. Uber die partiellen Differenzengliechungen der mathematisches Physik. *Math. Ann.*, 100:32–74, 1928.

[35] R Courant, K O Friedrichs, and H Lewy. On the partial difference equations of mathematical physics. *IBM Journal*, 11:215–235, 1967.

[36] M G Crandall, H Ishii, and P L Lions. User's guide to viscosity solutions of second order partial linear differential equations. *Bulletin of the American Math. Society*, 27:1–67, 1992.

[37] P Danielson. Euclidean distance mapping. *Computer Graphics and Image Processing*, 14:227–248, 1980.

[38] M P Do Carmo. *Differential Geometry of Curves and Surfaces.* Prentice-Hall Inc., New Jersey, 1976.

[39] L Dorst and K Trovato. Optimal path planning by cost wave propagating in metric configuration space. In *Proceedings of SPIE, Mobile Robots III*, volume 1007, pages 186–197, Cambridge, Massachusetts, November 1988.

[40] B A Dubrovin, A T Fomenko, and S P Novikov. *Modern Geometry - Methods and Applications I.* Springer-Verlag, New York, 1984.

[41] P Dupuis and J Oliensis. Direct method for reconstructing shape from shading. In *Proceedings IEEE CVPR*, pages 453–458, Champaign, Illinois, May 1992.

[42] P Dupuis and J Oliensis. An optimal control formulation and related numerical methods for a problem in shape reconstruction. Department of Computer Science COINS TR93-03, University of Massachusetts at Amherst, Amherst MA, 01003, 1993.

[43] C L Epstein and M Gage. The curve shortening flow. In A Chorin and A Majda, editors, *Wave Motion: Theory, Modeling, and Computation*. Springer-Verlag, New York, 1987.

[44] L C Evans and J Spruck. Motion of level sets by mean curvature, i. *J. Diff. Geom.*, 33, 1991.

[45] O Faugeras. On the evolution of simple curves of the real projective plane. *Comptes rendus de l'Acad. des Sciences de Paris*, 317:565–570, 1993.

[46] Feynman, Leighton, and Sands. *The Feynman Lectures on Physics*. Addison Westly, Massachusetts, 1964.

[47] P Fua and Y G Leclerc. Model driven edge detection. *Machine Vision and Applications*, 3:45–56, 1990.

[48] M Gage and R S Hamilton. The heat equation shrinking convex plane curves. *J. Diff. Geom.*, 23, 1986.

[49] P J Giblin and S A Brassett. Local symmetry of plane curves. *American Mathematical Monthly*, 92:689–707, 1985.

[50] M Gondran and M Minoux. *Graphs and Algorithms*. Wiley, Chichester, 1984. Ch. 2.

[51] M Grayson. The heat equation shrinks embedded plane curves to round points. *J. Diff. Geom.*, 26, 1987.

[52] M Grayson. Shortening embedded curves. *Annals of Mathematics*, 129:71–111, 1989.

[53] H B Griffiths. *Surfaces*. Cambridge University Press, Cambridge, 1981. Second Edition.

[54] A Harten, J M Hyman, and P D Lax. On finite-difference approximations and entropy conditions for shocks. *Comm. Pure Appl. Math.*, 29:297, 1976.

[55] B K P Horn. Obtaining shape from shading information. In P H Winston, editor, *The Psychology of Computer Vision*, pages 115–155. McGraw Hill, New York, 1987.

[56] B K P Horn. Height and gradient from shading. *International Journal of Computer Vision*, 5:37–75, 1990.

[57] B K P Horn and M J Brooks, editors. *Shape from Shading*. MIT Press, Cambridge MA, 1989.

[58] K Ikeuchi and B K P Horn. Numerical shape from shading and occluding boundaries. *Artificial Intelligence*, 17(1-3):141–184, 1981. Also in Horn and Brooks, 1989.

[59] K Kant and S Zucker. Towards efficient trajectory planning: The path–velocity decomposition. *The International Journal of Robotics Research*, 5(3):72–89, 1986.

[60] K Kant and S Zucker. Planning collision–free trajectories in time–varying environments: A two–level hierarchy. In *Proceedings International Conference on Robotics and Automation*, pages 1644–1649, 1988.

[61] M Kass, A Witkin, and D Terzopoulos. Snakes: Active contour models. *International Journal of Computer Vision*, 1:321–331, 1988.

[62] R Kimmel. Shape from shading via level sets. M.Sc. thesis (in Hebrew), Technion - Israel Institute of Technology, June 1992.

[63] R Kimmel, A Amir, and A M Bruckstein. Finding shortest paths on graph surfaces. Center for Intelligent Systems Report CIS #9301, Technion–Israel Institute of Technology, Israel, January 1993. presented in Curves and Surfaces, Chamonix, France, June 1993.

[64] R Kimmel, A Amir, and A M Bruckstein. Finding shortest paths on surfaces. In Méhautié Laurent and Schumaker, editors, *Curves and Surfaces in Geometric Design*, pages 259–268. A K Peters, Ltd., Wellesley, Massachusetts, 1994.

[65] R Kimmel, A Amir, and A M Bruckstein. Finding shortest paths on surfaces using level sets propagation. *IEEE Trans. on PAMI*, 17:to appear, June 1995.

[66] R Kimmel and A M Bruckstein. Shape from shading via level sets. Center for Intelligent Systems Report CIS #9209, Technion–Israel Institute of Technology, Israel, June 1992.

[67] R Kimmel and A M Bruckstein. Global shape from shading. Center for Intelligent Systems Report CIS #9327, Technion–Israel Institute of Technology, Israel, October 1993.

[68] R Kimmel and A M Bruckstein. Shape offsets via level sets. *CAD*, 25(5):154–162, March 1993.

[69] R Kimmel and A M Bruckstein. Sub-pixel distance maps and weighted distance transforms. In *Proceedings SPIE - Geometric Methods in Computer Vision II*, volume 2031, pages 259–268, San Diego, California, July 1993.

[70] R Kimmel and A M Bruckstein. Global shape from shading. In *Proceedings of ICPR, International Conference of Patternr Recognition*, pages 120–125, Jerusalem, Israel, October 1994.

[71] R Kimmel and A M Bruckstein. Global shape from shading. *CVIU*, to appear 1995.

[72] R Kimmel and A M Bruckstein. Tracking level sets by level sets: A method for solving the shape from shading problem. *CVIU*, 62(1):47–58, July 1995. presented in ICPR'94, Jerusalem, October, 1994.

[73] R Kimmel and N Kiryati. Finding shortest paths on surfaces by fast global approximation and precise local refinement. In *Proceedings of SPIE Vision Geometry III*, volume 2356, pages 198–209, Boston, Massachusetts, November 1994.

[74] R Kimmel, N Kiryati, and A M Bruckstein. Using multi-layer distance maps in finding shortest paths between moving obstacles. In *Proceedings of ICPR, International Conference of Pattern Recognition*, pages 367–372, Jerusalem, Israel, October 1994.

[75] R Kimmel, N Kiryati, and A M Bruckstein. Using multi-valued distance maps in finding shortest paths between moving obstacles. *submitted*, 1994.

[76] R Kimmel, N Kiryati, and A M Bruckstein. Distance maps and weighted distance transforms. *Journal of Mathematical Imaging and Vision, Special Issue on Topology and Geometry in Computer Vision*, to appear 1995.

[77] R Kimmel and G Sapiro. Shortening three dimensional curves via two dimensional flows. Center for Intelligent Systems Report CIS #9315, Technion–Israel Institute of Technology, Israel, April 1993.

[78] R Kimmel and G Sapiro. Shortening three dimensional curves via two dimensional flows. *International Journal: Computers & Mathematics with Applications*, 29(3):49–62, March 1995.

[79] R Kimmel, D Shaked, N Kiryati, and A M Bruckstein. Skeletonization via distance maps and level sets. In *Proceedings of SPIE Vision Geometry III*, volume 2356, pages 137–148, Boston, Massachusetts, November 1994.

[80] R Kimmel, D Shaked, N Kiryati, and A M Bruckstein. Skeletonization via distance maps and level sets. *CVIU*, to appear 1995.

[81] R Kimmel, K Siddiqi, B B Kimia, and A M Bruckstein. Shape from shading: Level set propagation and viscosity solutions. *International Journal of Computer Vision*, to appear 1995.

[82] N Kiryati and O Kübler. On chain code probabilities and length estimators for digitized three dimensional curves. *Pattern Recognition*, 28(3):361–372, 1995. Also Proc. 11th ICPR, The Hague, The Netherlands, Vol. A, pp. 259-262, August 30 - September 3, 1992.

[83] N Kiryati and G Székely. Estimating shortest paths and minimal distances on digitized three dimensional surfaces. *Pattern Recognition*, 26(11):1623–1637, 1993.

[84] P D Lax. *Hyperbolic Systems of Conservation Laws and the Mathematical Theory of Shock Waves*. Society for Industrial and Applied Mathematics, Philadelphia, Pennsylvania, 1973.

[85] C H Lee and A Rosenfeld. Improved methods of estimating shape from shading using the light source coordinate system. *Artificial Intelligence*, 26(1):125–143, May 1985.

[86] D T Lee. Medial axis transformation of a planar shape. *IEEE Trans. on PAMI*, 4:363–369, 1982.

[87] R J LeVeque. *Numerical Methods for Conservation Laws*. Lectures in Mathematics. Birkhauser Verlag, Basel, 1992.

[88] F Leymarie and M D Levine. Fast raster scan distance transform on the discrete rectangular lattice. *CVGIP: Image Understanding*, 55(1):84–94, 1992.

[89] F Leymarie and M D Levine. Simulating the grassfire transform using an active contour model. *IEEE Transactions on Pattern Analysis and Machine Intelligence*, 14(1):56–75, 1992.

[90] F Leymarie and M D Levine. Tracking deformable objects in the plane using an active contour model. *IEEE Transactions on Pattern Analysis and Machine Intelligence*, 15(6):617–634, 1993.

[91] M Leyton. Symmetry-curvature duality. *Computer Vision, Graphics, and Image Processing*, 38:327–341, 1987.

[92] P L Lions, E Rouy, and A Tourin. Shape-from-shading, viscosity solutions and edges. *Numerische Mathematik*, 64:323–353, 1993.

[93] R Malladi and J A Sethian. A unified framework for shape segmentation representation, and recognition. Lawrence Berkeley Lab. and Dep. of Math. LBL-36069 UC-405, Uni. of CA. Berkeley, August 1994.

[94] R Malladi, J A Sethian, and B C Vemuri. Evolutionary fronts for topology-independent shape modeling and recovery. In *Proceedings Third European Conference on Computer Vision*, pages 3–13, Stockholm, Sweden, May 1994.

[95] R Malladi, J A Sethian, and B C Vemuri. Shape modeling with front propagation: A level set approach. *IEEE Trans. on PAMI*, 17:158–175, 1995.

[96] J C Maxwell. On hills and dales. *Philos. Mag. (Maxwell's Collected Works)*, pages 233–240, 1870.

[97] F Meyer. Skeletons in digital spaces. In J Serra, editor, *Image Analysis and Mathematical Morphology, Vol. 2: Theoretical Advances*. Academic Press, San Diego California, 1988.

[98] J S B Mitchell, D M Mount, and C H Papadimitriou. The discrete geodesic problem. *SIAM J. Comput.*, 16(4):647–668, 1987.

[99] J S B Mitchell, D Payton, and D Keirsey. Planning and reasoning for autonomous vehicle control. *International Journal of Intelligent Systems*, 2:129–198, 1987.

[100] U Montanari. A method for obtaining skeletons using a quasi-Euclidean distance. *Journal of the Association for Computing Machinery*, 16(4):534–549, 1968.

[101] U Montanari. Continuous skeletons from digitized images. *Journal of the Association for Computing Machinery*, 16(4):534–549, 1969.

[102] W Mulder, S J Osher, and S J Sethian. Computing interface motion in compressible gas dynamics. *J. of Comp. Phys.*, 100:209–228, 1992.

[103] W Neuenschwander, P Fua, G Szekely, and O Kubler. Making snakes converge from minimal initialization. In *Proceedings of ICPR, International Conference of Pattern Recognition*, pages 613–615, Jerusalem, Israel, October 1994.

[104] R L Ogniewicz. *Discrete Voronoi Skeletons*. Hartung–Gorre Verlag Konstanz, Zürich, 1993.

[105] J Oliensis and P Dupuis. Direct method for reconstructing shape from shading. In *Proceedings SPIE Conf. 1570 on Geometric Methods in Computer Vision*, pages 116–128, 1991.

[106] J Oliensis and P Dupuis. A global algorithm for shape from shading. In *Proceedings 4th ICCV Conf.*, pages 692–701, Berlin, 1993.

[107] S Osher and L Rudin. Rapid convergence of approximate solutions to shape-from-shading problem. Technical report, Cognitech Inc., 1993. Unpublished.

[108] S Osher and C W Shu. High–order essentially nonoscillatory schemes for Hamilton–Jacobi equations. *SIAM J. Numer. Analy.*, 28(4):907–922, August 1991.

[109] S J Osher. A level set formulation for the solution of the Dirichlet problem for Hamilton–Jacobi equations. *SIAM J. Math. Anal.*, 24(5):1145–1152, September 1993.

[110] S J Osher and L I Rudin. Feature–oriented image enhancement using shock filters. *SIAM J. Numer. Analy.*, 27(4):919–940, August 1990.

[111] S J Osher and J A Sethian. Fronts propagating with curvature dependent speed: Algorithms based on Hamilton-Jacobi formulations. *J. of Comp. Phys.*, 79:12–49, 1988.

[112] A P Pentland. Local shading analysis. *IEEE Trans. on PAMI*, 6(2):170–187, 1984. Also in Horn and Brooks, 1989.

[113] A P Pentland. Linear shape from shading. *International Journal of Computer Vision*, 4:153–162, 1990.

[114] Y Pnueli and A M Bruckstein. DigiDurer - a digital engraving system. *The Visual Computer*, 10:277–292, 1994.

[115] Y Pnueli and A M Bruckstein. Gridless halftoning. *Submitted to Graphic Models and Image Processing*, 1994.

[116] S Riazanoff, B Cervelle, and J Chorowicz. Parametrisable skeletonization of binary and multi-level images. *Pattern Recognition Letters*, 11:25–33, January 1990.

[117] E Rouy and A Tourin. A viscosity solutions approach to shape-from-shading. *SIAM. J. Numer. Analy.*, 29(3):867–884, June 1992.

[118] D Rutovitz. Data structures for operations on digital images. In G C Cheng, R S Ledleyr, D K Pollock, and A Rosenfeld, editors, *Pictorial pattern recognition*, pages 105–133. Thompson Book, Washington, 1968.

[119] G Sapiro, R Kimmel, D Shaked, B Kimia, and A M Bruckstein. Implementing continuous–scale morphology via curve evolution. *Pattern Recognition*, 26(9):1363–1372, 1993.

[120] G Sapiro and A Tannenbaum. Affine invariant scale–space. *International Journal of Computer Vision*, 11(1):25–44, 1993.

[121] G Sapiro and A Tannenbaum. On invariant curve evolution and image analysis. *Indiana University Mathematics Journal*, 42(3), 1993.

[122] G Sapiro and A Tannenbaum. Area and length preserving geometric invariant scale-spaces. *IEEE Trans. on PAMI*, 17(1), 1995.

[123] Schroeder. The eikonal equation. *The Mathematical Intelligencer*, 5(1):36–37, 1983.

[124] E L Schwartz, A Shaw, and E Wolfson. A numerical solution to the generalized mapmaker's problem: Flattening non convex polyhedral surfaces. *IEEE Trans. on PAMI*, 11(9):1005–1008, 1989.

[125] J T Schwartz, M Sharir, and J Hopcroft, eds. *Planning, Geometry, and Complexity of Robot Motion*. Ablex Series in Artificial Intelligence. Ablex, Norwood, NJ, 1987.

[126] J A Sethian. Curvature and the evolution of fronts. *Commun. in Math. Phys.*, 101:487–499, 1985.

[127] J A Sethian. A review of recent numerical algorithms for hypersurfaces moving with curvature dependent speed. *J. of Diff. Geom.*, 33:131–161, 1989.

[128] J A Sethian and J Strain. Crystal growth and dendritic solidification. *J. of Computational Physics*, 98:231–253, 1992.

[129] D Shaked and A M Bruckstein. On symmetry axes and boundary curves. Center for Intelligent Systems Report CIS #9325, Technion–Israel Institute of Technology, Israel, 1993.

[130] D Shaked and A M Bruckstein. The curve axis. *CGIU*, to appear, 1995.

[131] M Sharir and A Schorr. On shortest paths in polyhedral spaces. *SIAM J. Comput.*, 1(15):193–215, 1986.

[132] J Smoller. *Shock Waves and Reaction-Diffusion Equations*. Springer-Verlag, New York, 1983.

[133] G A Sod. *Numerical Methods in Fluid Dynamics*. Cambridge Univ. Press, 1985.

[134] H M Soner. Motion of a set by the curvature of its boundary. *J. of Diff. Eq.*, 101, 1993.

[135] M Spivak. *A Comprehensive Introduction to Differential Geometry*. Publish or Perish, Inc., Berkeley, 1979.

[136] K Sugihara. Approximation of generalized Voronoi diagrams by ordinary Voronoi diagrams. *CVGIP: Graphical Models and Image Processing*, 55(6):522–531, 1993.

[137] M Sussman, P Smereka, and S J Osher. A level set approach for computing solutions to incompressible two-phase flow. Department of math., UCLA, Los Angeles, CA 90024-1555, June 1993.

[138] R Szeliski, D Tonnesen, and D Terzopoulos. Modeling surfaces of arbitrary topology with dynamic particles. In *Proceedings IEEE CVPR*, pages 82–87, 1993.

[139] D Terzopoulos. On matching deformable models to images. In *Topical meeting on machine vision, Technical Digest Series, Optical Society of America*, volume 12, pages 160–163, 1987.

[140] D Terzopoulos, A Witkin, and M Kass. Constraints on deformable models: Recovering 3d shape and nonrigid motions. *Artificial Intelligence*, 36:91–123, 1988.

[141] P W Verbeek and B J H Verwer. Shading from shape, the eikonal equation solved by gray-weighted distance transform. *Pattern Recognition Letters*, 11:681–690, 1990.

[142] B J H Verwer, L J Van Vliet, and P W Verbeek. Binary and gray-value skeletons: Metrics and algorithms. *International Journal of Pattern Recognition and Artificial Intelligence*, 7(5):1287–1308, 1993.

[143] L Vincent. Exact euclidean distance function by chain propagation. In *Proceedings IEEE CVPR*, pages 520–525, May 1991.

[144] E Wolfson and E L Schwartz. Computing minimal distances on polyhedral surfaces. *IEEE Trans. on PAMI*, 11(9):1001–1005, 1989.

[145] S D Yanowitz and A M Bruckstein. A new method for image segmentation. *Computer Vision, Graphics, and Image Processing*, 46:82–95, 1989.